Applied Mathematics and Computation 364 (2020) 124669

Contents lists available at ScienceDirect

Applied Mathematics and Computation

journal homepage: www.elsevier.com/locate/amc

Closed-form approximate solutions for a class of coupled nonlinear stochastic differential equations

Antonios T. Meimaris[a], Ioannis A. Kougioumtzoglou[b], Athanasios A. Pantelous[a,*]

[a] Department of Econometrics and Business Statistics, Monash Business School, Monash University, 20 Chancellors Walk, Wellington Rd, Clayton, VIC 3800, Australia

[b] Department of Civil Engineering and Engineering Mechanics, The Fu Foundation School of Engineering and Applied Science, Columbia University, 500 West 120th Street, New York, NY 10027, USA

ARTICLE INFO

Keywords:
Nonlinear stochastic dynamics
Path Integral
Error quantification
Cauchy–Schwarz inequality
Fokker–Planck equation
Stochastic differential equations

ABSTRACT

An approximate solution technique is developed for a class of coupled multi-dimensional stochastic differential equations with nonlinear drift and constant diffusion coefficients. Relying on a Wiener path integral formulation and employing the Cauchy–Schwarz inequality, an approximate closed-form expression for the joint response process transition probability density function is determined. Next, the accuracy of the approximation is further enhanced by proposing a more versatile closed-form expression with additional "degrees of freedom"; that is, parameters to be determined. To this aim, an error minimization problem related to the corresponding Fokker–Planck equation is formulated and solved. Several diverse numerical examples are considered for demonstrating the reliability of the herein developed solution technique, which requires minimal computational cost for determining the joint response transition probability density function and exhibits satisfactory accuracy as compared with pertinent Monte Carlo simulation data.

1. Introduction

Systems of coupled nonlinear ordinary stochastic differential equations (SDEs) are widely used for modeling the dynamics of diverse systems. In this regard, several solution methodologies have been developed in the literature, with Monte Carlo (MC) simulation techniques [1,2] being among the most widely utilized numerical approaches. Nevertheless, in certain situations MC techniques can be computationally highly intensive, and thus, a need for developing alternative approximate solution methodologies arises; see, for instance, some indicative work in the field of chemical processes (e.g., [3,4]). Further, based on preliminary work in [5], Naess and co-workers developed a stochastic response determination numerical scheme by utilizing a discrete version of the Chapman–Kolmogorov equation, and by propagating the response probability density function (PDF) in short time steps [6,7]. Nevertheless, although the scheme exhibits excellent accuracy in predicting even the tails of the system response PDF, it becomes eventually computationally prohibitive with increasing dimensionality. This is due to the fact that a multi-convolution integral needs to be computed for each and every time step, while the time increment is required to be short. The reader is also referred to [8,9] for other alternative approximate techniques for solving SDEs modelling the random vibrations of diverse structural and mechanical systems.

* Corresponding author.
E-mail addresses: Antonios.Meimaris@monash.edu (A.T. Meimaris), ikougioum@columbia.edu (I.A. Kougioumtzoglou), Athanasios.Pantelous@monash.edu (A.A. Pantelous).

https://doi.org/10.1016/j.amc.2019.124669
0096-3003/

Recently, Kougioumtzoglou and co-workers developed a semi-analytical technique based on the concept of the Wiener path integral (WPI) [10,11] for determining the joint response PDF of coupled nonlinear SDEs describing the dynamics of multi-degree-of-freedom structural systems subject to stochastic excitation [12–15]. In general, although the WPI technique has exhibited both versatility and relatively high accuracy in addressing a wide range of engineering problems (e.g. [16–18]), its implementation relates, unfortunately, to non-negligible computational cost; see [15,19] for more details and some recent enhancements of the technique regarding computational efficiency. Motivated by the above challenge, and relying on a WPI formulation, as well as on a Cauchy–Schwarz inequality treatment, the authors derived recently in [20,21] closed-form approximate expressions for the response PDF of a class of one-dimensional nonlinear SDEs. Due to the analytical nature of the solution techniques, minimal computational effort is required, while the approximate PDF has demonstrated satisfactory accuracy as compared to pertinent Euler–Maruyama MC simulation data.

In this paper, the approximations proposed in [20,21] are generalized to account for multi-dimensional stochastic processes related to systems of coupled nonlinear Itô SDEs. Specifically, first, a basic approximation is derived for the joint response transition PDF, which is enhanced further by introducing additional "degrees-of-freedom", i.e., parameters to be determined. To this aim, an error minimization problem associated with the corresponding Fokker–Planck equation is formulated and solved. This enhancement aims at "tightening" the Cauchy-Schwarz inequality as well as increasing the overall accuracy of the basic approximation. Several diverse numerical examples are considered for demonstrating the reliability of the approximation, while comparisons with Euler–Maruyama MC data demonstrate a satisfactory degree of accuracy.

The outline of the paper is as follows: In Section 2, the basic aspects of the WPI technique are delineated, while a note regarding the Cauchy–Schwarz inequality is included as well. In Section 3, a closed-form approximate joint response transition PDF for a class of multi-dimensional coupled SDEs with nonlinear drift and constant diffusion coefficients is derived, which is supplemented by an error quantification analysis as well. This, in turn, facilitates the development of an enhanced approximate joint PDF by proposing a more versatile closed-form expression with additional parameters to be determined by resorting to an appropriate error minimization scheme. Section 4 corresponds to the numerical examples, while concluding remarks are provided in Section 5.

2. Preliminaries

Let $(\Omega, \mathcal{F}, \mathcal{F}_{t\geq 0}, \mathbb{P})$ be a complete filtered probability space on which a scalar standard Brownian motion $(B_t,\ t\geq 0)$ is defined, and $\mathcal{F}_t$ is the augmentation of $\sigma\{B_s|0\leq s\leq t\}$ by all the $\mathbb{P}$-null sets of $\mathcal{F}$.

2.1. Wiener path integral overview

In general, for an N-dimensional stochastic process $\mathbf{X}_t = \left(X^{(1)}(t),\ X^{(2)}(t),\ldots,\ X^{(N)}(t)\right)$ the joint transition PDF $p(\mathbf{x}_f, t_f|\mathbf{x}_i, t_i)$ from a point in state space $\mathbf{x}_i$ at time t_i to a point $\mathbf{x}_f$ at time t_f, where $t_f > t_i$, can be expressed as a functional integral over the space of all possible paths $C\{\mathbf{x}_i, t_i; \mathbf{x}_f, t_f\}$ in the form (e.g., see [15])

$$p\left(\mathbf{x}_f, t_f|\mathbf{x}_i, t_i\right) = \int_{\{\mathbf{x}_i,t_i\}}^{\{\mathbf{x}_f,t_f\}} \Xi[\mathbf{x}(t)][d\mathbf{x}(t)]. \tag{1}$$

In Eq. (1), $\Xi[\mathbf{x}(t)]$ represents the probability density functional, which can be explicitly determined in closed-form only for relatively simple cases of stochastic processes, and $[d\mathbf{x}(t)]$ represents a functional measure. For instance, for a Gaussian white noise process vector $\mathbf{w}(t)$ possessing a diagonal power spectrum matrix

$$\mathbf{S} = \begin{bmatrix} S_0 & & \\ & \ddots & \\ & & S_0 \end{bmatrix}, \tag{2}$$

$\Xi[\mathbf{x}(t)]$ is given by [22]

$$\Xi[\mathbf{w}(t)] = \exp\left[-\int_{t_i}^{t_f} \frac{1}{4\pi}\mathbf{w}(t)^T\mathbf{S}^{-1}\mathbf{w}(t)dt\right]. \tag{3}$$

Without loss of generality and for notation simplicity, it has been assumed that the constant entries of the power spectrum matrix of Eq. (2) are identical, and equal to S_0. A detailed derivation and discussion of Eq. (3) can be found in standard path integral related books such as [23]. In the ensuing analysis, the following system of coupled nonlinear Itô stochastic differential equations is considered, i.e.,

$$dX_t^{(j)} = \mu_j(\mathbf{X}_t)dt + \sigma dB_t^{(j)},\quad \forall j \in \{1, 2, \ldots, N\} \equiv \lceil N \rfloor, \tag{4}$$

where $\mu(\mathbf{X}_t) = (\mu_1(\mathbf{X}_t), \mu_2(\mathbf{X}_t), \ldots, \mu_N(\mathbf{X}_t))^T$ denotes the nonlinear drift coefficient vector, $\sigma^2 = 2\pi S_0$ is the constant diffusion coefficient, and dB/dt represents the formal time-derivative of a white noise process of unit intensity. In this regard, Eq. (4) can be substituted into Eq. (3), yielding for the transition PDF of the response process $\mathbf{X}_t$ the expression (e.g., see

[12–16])

$$p\left(\mathbf{x}_f, t_f|\mathbf{x}_i, t_i\right) = \int_{\{\mathbf{x}_i,t_i\}}^{\{\mathbf{x}_f,t_f\}} \exp\left(-\int_{t_i}^{t_f} L(\mathbf{x}, \dot{\mathbf{x}})dt\right)[d\mathbf{x}(t)], \tag{5}$$

where $L(\mathbf{x}, \dot{\mathbf{x}})$ represents the Lagrangian function associated with the dynamical system of Eq. (4), and is given by

$$L(\mathbf{x}, \dot{\mathbf{x}}) = \frac{1}{2\sigma^2}\sum_{j=1}^{N}\left(\dot{x}^{(j)} - \mu_j(\mathbf{x})\right)^2. \tag{6}$$

As noted earlier, the constant diffusion coefficients in Eq. (5) are taken all equal to σ for convenience and notation simplicity. It is rather straightforward to consider non-equal values for the diffusion coefficients in Eq. (5) (corresponding to non-equal entries in the power spectrum matrix of Eq. (2)) and adjust accordingly Eq. (6). Further, although the assumption of constant diffusion coefficients appears rather restrictive, it is often possible to transform more general cases with state-dependent/nonlinear diffusion coefficients into the form of Eq. (5); see for instance [24], as well as the herein considered example in Section 4.3. Furthermore, the assumption of constant diffusion may be quite reasonable for various engineering dynamics applications. Indicatively, the SDE governing the dynamics of a class of oscillators with nonlinear damping subject to stochastic excitation can be approximated via a stochastic averaging treatment by Eq. (4); see, for instance, the numerical examples in [12] for more details. Extending the herein developed solution technique for the more general and significantly more challenging case of nonlinear drift and nonlinear diffusion coefficients is identified as future work.

Next, it is readily seen that, in general, the analytical evaluation of the WPI, Eq. (5), is at least a rather challenging, if not impossible, task. Thus, seeking for an approximate solution technique, it is observed that the greatest contribution to the WPI comes from the trajectory for which the integral in the exponential of Eq. (5) becomes as small as possible. According to calculus of variations [25], this trajectory with fixed end points satisfies the extremality condition

$$\delta\int_{t_i}^{t_f} L(\mathbf{x}_c, \dot{\mathbf{x}}_c)dt = 0, \tag{7}$$

where $\mathbf{x}_c$ denotes the "*most probable path*" to be determined by the functional optimization problem

$$Min(Max) \qquad J[\mathbf{x}_c(t)] = \int_{t_i}^{t_f} L(\mathbf{x}_c, \dot{\mathbf{x}}_c)dt, \tag{8}$$

together with the boundary conditions $\mathbf{x}_c(t_i) = \mathbf{x}_i$ and $\mathbf{x}_c(t_f) = \mathbf{x}_f$. Further, $\mathbf{x}_c(t)$ can be determined either by deriving and solving a system of Euler–Lagrange (E–L) equations associated with Eq. (7) (e.g., see [13,15]), i.e.

$$\frac{\partial L}{\partial x_c^{(k)}} - \frac{\partial}{\partial t}\frac{\partial L}{\partial \dot{x}_c^{(k)}} = 0, \forall k \in \lceil N \rfloor, \tag{9}$$

in conjunction with the boundary conditions $\mathbf{x}_c(t_i) = \mathbf{x}_i$, $\mathbf{x}_c(t_f) = \mathbf{x}_f$, or alternatively, by treating directly the deterministic boundary value problem (BVP) of Eq. (8) (e.g. [14,16]). Once $\mathbf{x}_c(t)$ is determined, the joint transition PDF can be approximated by

$$p\left(\mathbf{x}_f, t_f|\mathbf{x}_i, t_i\right) \approx \Phi\exp\left(-\int_{t_i}^{t_f} L(\mathbf{x}_c, \dot{\mathbf{x}}_c)dt\right), \tag{10}$$

where Φ is a normalization coefficient.

2.2. Cauchy–Schwarz inequality

For completeness, the integral form of the Cauchy–Schwarz inequality is included below, whereas a detailed presentation of the topic can be found in [26].

Lemma 2.1. *Let f and g be real functions that are continuous on the closed interval $[a, b]$. Then*

$$\left(\int_a^b f(t)g(t)dt\right)^2 \le \int_a^b f(t)^2dt\int_a^b g(t)^2dt. \tag{11}$$

Clearly, setting $g = 1$ yields the special case

$$\int_a^b f(t)^2dt \ge \frac{1}{b-a}\left(\int_a^b f(t)dt\right)^2, \tag{12}$$

which will be used in Section 3.1 for proving Lemma 3.1.

3. Main results

3.1. A closed-form approximate solution for stochastically driven nonlinear dynamical systems with constant diffusion

Although the approximate expression of Eq. (10) has exhibited a significant degree of accuracy (as compared to pertinent MC simulation data) in several applications such as those pertaining to engineering dynamical systems [14,15,20], there is a considerable computational cost associated with solving numerically the BVPs of Eq. (8); see for instance [19] for a recent work towards enhancing the computational efficiency of the WPI. In this section, a closed-form approximate expression for the joint response transition PDF of Eq. (4) is derived by relying on a Cauchy–Schwarz inequality treatment. The approximate solution, which can be construed as a generalization of the results of [20] to account for multi-dimensional processes $\mathbf{X}_t$, not only requires essentially zero computational effort, but also facilitates an error quantification analysis (see Section 3.2).

Regarding the system of coupled nonlinear SDEs of Eq. (4), the following Lemma is proved next, which will be instrumental in deriving the approximate joint response PDF.

Lemma 3.1. *Let $M^{(j)}(\cdot)$ be an antiderivative of $\mu_j(\cdot)\forall j$ w.r.t the jth coordinate, i.e.,*

$$\frac{\partial M^{(j)}(\mathbf{x})}{\partial x^{(j)}} = \mu_j(\mathbf{x}) \ \forall j. \tag{13}$$

Then, the integral of the Lagrangian function, $\int_{t_i}^{t_f} L(\mathbf{x}_c, \dot{\mathbf{x}}_c)dt$, is bounded by

$$\int_{t_i}^{t_f} L(\mathbf{x}_c, \dot{\mathbf{x}}_c)dt \geq \frac{1}{2\sigma^2}\left(\sum_{j=1}^{N}\frac{\left(\chi^{(j)}\right)^2}{\tau} - b\tau - 2\sum_{j=1}^{N}\left(M^{(j)}(\mathbf{x}_f) - M^{(j)}(\mathbf{x}_i)\right)\right), \tag{14}$$

where $\chi^{(j)} = x_f^{(j)} - x_i^{(j)}$, $\tau = t_f - t_i$ and b is a constant, depending on the boundary conditions $\mathbf{x}_c(t_i) = \mathbf{x}_i$, $\mathbf{x}_c(t_f) = \mathbf{x}_f$.

Proof. Substituting the Lagrangian function of Eq. (6) corresponding to the system of SDEs of Eq. (4) into the E–L Eq. (9), and manipulating, yields

$$-\frac{1}{\sigma^2}\sum_{j=1}^{N}\left(\dot{x}_c^{(j)} - \mu_j(\mathbf{x}_c)\right)\frac{\partial \mu_j(\mathbf{x}_c)}{\partial x_c^{(k)}} - \frac{1}{\sigma^2}\left(\ddot{x}_c^{(k)} - \sum_{j=1}^{N}\frac{\partial \mu_k(\mathbf{x}_c)}{\partial x_c^{(j)}}\dot{x}_c^{(j)}\right) = 0, \forall k \in \lceil N \rfloor, \tag{15}$$

together with the boundary conditions $\mathbf{x}_c(t_i) = \mathbf{x}_i$, $\mathbf{x}_c(t_f) = \mathbf{x}_f$. Further, Eq. (15) can be cast in the form

$$\ddot{x}_c^{(k)} = \sum_{j=1}^{N}\dot{x}_c^{(j)}\left(\frac{\partial \mu_k(\mathbf{x}_c)}{\partial x_c^{(j)}} - \frac{\partial \mu_j(\mathbf{x}_c)}{\partial x_c^{(k)}}\right) + \sum_{j=1}^{N}\mu_j(\mathbf{x}_c)\frac{\partial \mu_j(\mathbf{x}_c)}{\partial x_c^{(k)}}, \forall k \in \lceil N \rfloor, \tag{16}$$

or equivalently written as

$$\frac{\partial}{\partial t}\left(\left(\dot{x}_c^{(k)}\right)^2\right) = 2\sum_{j=1}^{N}\dot{x}_c^{(j)}\left(\frac{\partial \mu_k(\mathbf{x}_c)}{\partial x_c^{(j)}} - \frac{\partial \mu_j(\mathbf{x}_c)}{\partial x_c^{(k)}}\right)\dot{x}_c^{(k)} + \sum_{j=1}^{N}2\mu_j(\mathbf{x}_c)\frac{\partial \mu_j(\mathbf{x}_c)}{\partial x_c^{(k)}}\dot{x}_c^{(k)}, \forall k \in \lceil N \rfloor. \tag{17}$$

Considering Eq. (17), and summing over all k indexes yields

$$\sum_{k=1}^{N}\frac{\partial}{\partial t}\left(\left(\dot{x}_c^{(k)}\right)^2\right) = 2\sum_{k=1}^{N}\sum_{j=1}^{N}\dot{x}_c^{(j)}\left(\frac{\partial \mu_k(\mathbf{x}_c)}{\partial x_c^{(j)}} - \frac{\partial \mu_j(\mathbf{x}_c)}{\partial x_c^{(k)}}\right)\dot{x}_c^{(k)} + \sum_{k=1}^{N}\sum_{j=1}^{N}2\mu_j(\mathbf{x}_c)\frac{\partial \mu_j(\mathbf{x}_c)}{\partial x_c^{(k)}}\dot{x}_c^{(k)}, \tag{18}$$

or equivalently,

$$\sum_{k=1}^{N}\frac{\partial}{\partial t}\left(\left(\dot{x}_c^{(k)}\right)^2\right) = \sum_{j=1}^{N}2\mu_j(\mathbf{x}_c)\sum_{k=1}^{N}\frac{\partial \mu_j(\mathbf{x}_c)}{\partial x_c^{(k)}}\dot{x}_c^{(k)}, \tag{19}$$

since by symmetry,

$$\sum_{k=1}^{N}\sum_{j=1}^{N}\dot{x}_c^{(j)}\left(\frac{\partial \mu_k(\mathbf{x}_c)}{\partial x_c^{(j)}} - \frac{\partial \mu_j(\mathbf{x}_c)}{\partial x_c^{(k)}}\right)\dot{x}_c^{(k)} = 0. \tag{20}$$

Taking into account the chain rule of differentiation, Eq. (19) becomes

$$\sum_{k=1}^{N}\frac{\partial}{\partial t}\left(\left(\dot{x}_c^{(k)}\right)^2\right) = \sum_{j=1}^{N}2\mu_j(\mathbf{x}_c)\frac{\partial}{\partial t}\mu_j(\mathbf{x}_c) = \sum_{j=1}^{N}\frac{\partial}{\partial t}\left(\mu_j(\mathbf{x}_c)^2\right), \tag{21}$$

or equivalently,

$$\frac{\partial}{\partial t}\left(\sum_{k=1}^{N}\left(\dot{x}_c^{(k)}\right)^2\right)=\frac{\partial}{\partial t}\left(\sum_{j=1}^{N}\mu_j(\mathbf{x}_c)^2\right), \tag{22}$$

which yields

$$\sum_{k=1}^{N}\left(\dot{x}_c^{(k)}\right)^2=\sum_{j=1}^{N}\mu_j(\mathbf{x}_c)^2+b. \tag{23}$$

In Eq. (23) b is a constant, depending on the boundary conditions $\mathbf{x}_c(t_i)=\mathbf{x}_i,\ \mathbf{x}_c(t_f)=\mathbf{x}_f$. Expanding next the square in Eq. (6), and substituting Eq. (23) yields

$$L(\mathbf{x}_c,\dot{\mathbf{x}}_c)=\frac{1}{2\sigma^2}\left(2\sum_{j=1}^{N}\left(\dot{x}_c^{(j)}\right)^2-b-2\sum_{j=1}^{N}\mu_j(\mathbf{x}_c)\dot{x}_c^{(j)}\right). \tag{24}$$

Next, the integral of Eq. (24) is given by

$$\int_{t_i}^{t_f}L(\mathbf{x}_c,\dot{\mathbf{x}}_c)dt=\frac{1}{2}\left(\frac{\sum_{j=1}^{N}2\int_{t_i}^{t_f}\left(\dot{x}_c^{(j)}\right)^2dt-b\tau-2\sum_{j=1}^{N}\int_{t_i}^{t_f}\mu_j(\mathbf{x}_c)dx_c^{(j)}}{\sigma^2}\right), \tag{25}$$

or equivalently, by utilizing the $M^{(j)}$ antiderivatives of Eq. (13)

$$\int_{t_i}^{t_f}L(\mathbf{x}_c,\dot{\mathbf{x}}_c)dt=\frac{1}{2}\left(\frac{\sum_{j=1}^{N}2\int_{t_i}^{t_f}\left(\dot{x}_c^{(j)}\right)^2dt-b\tau-2\sum_{j=1}^{N}\left(M^{(j)}(\mathbf{x}_f)-M^{(j)}(\mathbf{x}_i)\right)}{\sigma^2}\right). \tag{26}$$

Further, employing the Cauchy–Schwarz inequality of Eq. (12), the quantity $2\int_{t_i}^{t_f}\left(\dot{x}_c^{(j)}\right)^2dt$ is bounded by

$$2\int_{t_i}^{t_f}\left(\dot{x}_c^{(j)}\right)^2dt\geq\int_{t_i}^{t_f}\left(\dot{x}_c^{(j)}\right)^2dt\geq\frac{\left(x_f^{(j)}-x_i^{(j)}\right)^2}{\tau}=\frac{\left(\chi^{(j)}\right)^2}{\tau}. \tag{27}$$

Combining Eqs. (26) and (27), Eq. (14) is derived. □

In the following, the main result of the present section is stated and proved.

Theorem 3.2. *Let*

$$G\left(\mathbf{x}_f,t_f|\mathbf{x}_i,t_i\right)=\frac{\sum_{j=1}^{N}\left(\chi^{(j)}\right)^2+\sum_{j=1}^{N}\left(-2M^{(j)}(\mathbf{x}_f)+2M^{(j)}(\mathbf{x}_i)\right)\tau}{2\tau\sigma^2}, \tag{28}$$

then an approximate joint transition PDF for Eq. (4) is given by $\hat{p}:\mathcal{D}(M)\times(t_i,+\infty)\times\{\mathbf{x}_i\}\times\{t_i\}\to\mathbb{R}$, *where* $\mathcal{D}(M)=\mathcal{D}(M^{(1)})\times\mathcal{D}(M^{(2)})\times\cdots\times\mathcal{D}(M^{(N)})$, *defined as*

$$\hat{p}\left(\mathbf{x}_f,t_f|\mathbf{x}_i,t_i\right)=F(t_f)\exp\left(-G\left(\mathbf{x}_f,t_f|\mathbf{x}_i,t_i\right)\right), \tag{29}$$

where $F(t_f)$ *is a normalization constant.*

Proof. The proof follows in a straightforward manner from Lemma 3.1 and Eqs. (10) and (14). Thus, it can be readily seen that a closed-form approximate solution for the joint transition PDF can be given by Eq. (29), where $F(t_f)=\left(\int_{\mathcal{D}(M)}exp\left(-G\left(\mathbf{x},t_f|\mathbf{x}_i,t_i\right)\right)d\mathbf{x}\right)^{-1}$. Note that the arbitrary term $\exp\left(\frac{-b\tau}{2\sigma^2}\right)$ has been included in the constant $F(t_f)$. □

3.2. Error quantification

The transition PDF of Eq. (29) derived herein constitutes an approximate solution of the coupled system of nonlinear SDEs of Eq. (4). Naturally, the next step is to quantify the accuracy of the derived approximation and estimate its error. In this regard, for a given norm ($\|\cdot\|_q$), the error quantity $\|\hat{p}-p^*\|_q$ can be defined, where p^* is the exact transition PDF. Clearly, however, the error quantity $\|\hat{p}-p^*\|_q$ cannot be determined explicitly as p^* is unknown. Thus, an alternative error definition, also adopted in [20,21], is utilized in the ensuing analysis. Specifically, the transition PDF p^* for the SDEs of Eq. (4) is given as the solution of the associated Fokker–Planck equation [27], i.e.,

$$\exists p^*:\frac{\partial p^*(\mathbf{x},t)}{\partial t}=-\sum_{j=1}^{N}\frac{\partial\left(\mu_j(\mathbf{x})p^*(\mathbf{x},t)\right)}{\partial x^{(j)}}+\frac{\sigma^2}{2}\sum_{j=1}^{N}\sum_{k=1}^{N}\frac{\partial^2p^*(y,t)}{\partial x^{(j)}\partial x^{(k)}}. \tag{30}$$

Let us denote the Fokker–Planck operator as follows

$$\mathcal{L}_{FP}[p(\mathbf{x},t)] = \frac{\partial p(\mathbf{x},t)}{\partial t} + \sum_{j=1}^{N} \frac{\partial\left(\mu_j(\mathbf{x})p(\mathbf{x},t)\right)}{\partial x^{(j)}} - \frac{\sigma^2}{2}\sum_{j=1}^{N}\sum_{k=1}^{N}\frac{\partial^2 p(\mathbf{x},t)}{\partial x^{(j)}\partial x^{(k)}}. \tag{31}$$

From Eq. (30), it follows that $L_{FP}[p^*] = 0$. Thus, the error is defined as $\|\mathcal{L}_{FP}[\hat{p} - p^*]\|_q = \|\mathcal{L}_{FP}[\hat{p}] - \mathcal{L}_{FP}[p^*]\|_q = \|\mathcal{L}_{FP}[\hat{p}]\|_q$ (see also [20,21]).

Clearly, utilizing the Fokker–Planck operator in the above error definition (see also [28–30]) facilitates the evaluation via $\|\mathcal{L}_{FP}[\hat{p}]\|_q$ of the error incurred by using $\hat{p}$ as an approximation to the exact PDF p^*. In particular, substituting the approximate transition PDF of Eq. (29) into Eq. (31) and manipulating yields

$$\mathcal{L}_{FP}[\hat{p}] = \hat{p}\left(\frac{\dot{F}}{F} - \frac{\partial G}{\partial t} + \sum_{j=1}^{N}\left(\frac{\mu_j}{\partial x^{(j)}} - \mu_j\frac{\partial G}{\partial x^{(j)}}\right) - \frac{\sigma^2}{2}\sum_{j=1}^{N}\sum_{k=1}^{N}\left(-\frac{\partial^2 G}{\partial x^{(j)}\partial x^{(k)}} + \left(\frac{\partial G}{\partial x^{(j)}}\right)\left(\frac{\partial G}{\partial x^{(k)}}\right)\right)\right). \tag{32}$$

Differentiating Eq. (28) leads to

$$-\frac{\partial G}{\partial t}\Big|_{\mathbf{x}=\mathbf{x}_f,t=t_f} = \frac{1}{2\sigma^2}\sum_{j=1}^{N}\left(\frac{\chi^{(j)}}{\tau}\right)^2, \tag{33}$$

$$\frac{\partial G}{\partial x^{(j)}}\Big|_{\mathbf{x}=\mathbf{x}_f,t=t_f} = \frac{\frac{x_f^{(j)}-x_i^{(j)}}{\tau} - \mu_j(\mathbf{x}_f)}{\sigma^2}, \tag{34}$$

$$\frac{\partial^2 G}{\partial x^{(j)}\partial x^{(k)}}\Big|_{\mathbf{x}=\mathbf{x}_f,t=t_f} = \left(\frac{\partial}{\partial x^{(j)}}\left(\frac{\partial G}{\partial x^{(k)}}\right)\right)\Big|_{\mathbf{x}=\mathbf{x}_f,t=t_f} = \frac{\mathbf{1}_{j=k} - \frac{\partial}{\partial x^{(j)}}\mu_k(\mathbf{x}_f))\tau}{\tau\sigma^2}. \tag{35}$$

Next, substituting Eqs. (33) to (35) into Eq. (32), and manipulating, yields

$$\begin{aligned}\mathcal{L}_{FP}[\hat{p}] = \frac{\hat{p}\left(\mathbf{x}_f,t_f|\mathbf{x}_i,t_i\right)}{2}\Bigg(&2\frac{\dot{F}(t_f)}{F(t_f)} + \frac{N}{\tau} + \frac{1}{\sigma^2}\sum_{j=1}^{N}\mu_j(\mathbf{x}_f)^2 + \sum_{j=1}^{N}\frac{\partial\mu_j(\mathbf{x}_f)}{\partial x^{(j)}}\\ &- \sum_{j\neq k}\frac{\partial\mu_k(\mathbf{x}_f)}{\partial x^{(j)}} - \frac{1}{\sigma^2}\sum_{j\neq k}\left(\frac{\chi^{(j)}}{\tau} - \mu_j(\mathbf{x}_f)\right)\left(\frac{\chi^{(k)}}{\tau} - \mu_k(\mathbf{x}_f)\right)\Bigg).\end{aligned} \tag{36}$$

Utilizing Eq. (36), the error function, $err(\mathbf{x}_f, t_f|\mathbf{x}_i, t_i)$, and its normalized version are given by

$$\begin{aligned}err\left(\mathbf{x}_f,t_f|\mathbf{x}_i,t_i\right) = \Bigg\|\frac{\hat{p}\left(\mathbf{x}_f,t_f|\mathbf{x}_i,t_i\right)}{2}\Bigg(&2\frac{\dot{F}(t_f)}{F(t_f)} + \frac{N}{\tau} + \sum_{j=1}^{N}\frac{\partial\mu_j(\mathbf{x}_f)}{\partial x^{(j)}} - \sum_{j\neq k}\frac{\partial\mu_k(\mathbf{x}_f)}{\partial x^{(j)}}\\ &+ \frac{1}{\sigma^2}\sum_{j=1}^{N}\mu_j(\mathbf{x}_f)^2 - \frac{1}{\sigma^2}\sum_{j\neq k}\left(\frac{\chi^{(j)}}{\tau} - \mu_j(\mathbf{x}_f)\right)\left(\frac{\chi^{(k)}}{\tau} - \mu_k(\mathbf{x}_f)\right)\Bigg)\Bigg\|_q\end{aligned} \tag{37}$$

and

$$\widetilde{err}\left(\mathbf{x}_f,t_f|\mathbf{x}_i,t_i\right) = \frac{err\left(\mathbf{x}_f,t_f|\mathbf{x}_i,t_i\right)}{\sup\limits_{\substack{\mathbf{x}_f\in\mathcal{D}(M)\\ t_f\in[t_i^+,+\infty)}} err\left(\mathbf{x}_f,t_f|\mathbf{x}_i,t_i\right)}, \tag{38}$$

where $\sup(\cdot)$ denotes the supremum operator.

Overall, the normalized error of Eq. (38) can be estimated for a given system of SDEs of Eq. (4) for assessing the relative accuracy of the approximate response transition PDF both for various x_f values, and for various time instants t_f.

3.3. SDEs with constant drift and diffusion coefficients: an exact analytical solution case

For the special case of constant drift coefficients, the system of coupled SDEs of Eq. (4) degenerates to

$$dX_t^{(j)} = \mu_j dt + \sigma dB_t^{(j)}, \quad \forall j \in \lceil N \rfloor, \tag{39}$$

Eq. (39) represents a system of uncoupled SDEs, which has been used, for instance, to model the motion of particles [31]. In this regard, the approximate PDF of Eq. (29) takes the form (see also [20])

$$\hat{p}\left(\mathbf{x}_f,t_f|\mathbf{x}_i,t_i\right) = F(t_f)\exp\left(-\frac{\sum_{j=1}^{N}\left(\chi^{(j)}\right)^2 + \sum_{j=1}^{N}\left(-2\mu x_f^{(j)} + 2\mu x_i^{(j)}\right)\tau}{2\tau\sigma^2}\right), \tag{40}$$

or equivalently,

$$\hat{p}\left(\mathbf{x}_f, t_f|\mathbf{x}_i, t_i\right) = \tilde{F}(t_f)\exp\left(-\sum_{j=1}^{N}\frac{\left(\chi^{(j)}-\mu\tau\right)^2}{2\tau\sigma^2}\right), \tag{41}$$

where the term $\exp\left(\frac{N\mu^2\tau^2}{2\tau\sigma^2}\right)$ has been merged with the normalization coefficient $\tilde{F}(t_f)$. Note that for the SDEs of Eq. (39), an exact response PDF for the process $\mathbf{X}(t)$ is available (e.g., [32]) which, notably, coincides with Eq. (41). Also, it can be readily seen that substituting Eq. (41) into Eq. (37) yields $err(\mathbf{x}_f, t_f|\mathbf{x}_i, t_i) = 0$, and thus, as anticipated, the error of approximating the exact PDF of Eq. (39) with the approximate one of Eq. (29) is zero, since in that case the two PDFs coincide as discussed earlier.

3.4. Enhanced accuracy via an error minimization scheme

It can be readily seen that $\hat{p}$ in Eq. (29) can be directly used as an analytical approximation of the joint response process PDF without resorting to the numerical solution of the E–L Eq. (9). Thus, essentially zero computational effort is required for the determination of the joint response transition PDF. However, as demonstrated in [20] for the one-dimensional case, although the approximation of Eq. (29) is capable, in general, of capturing the salient features of the solution PDF, in many cases the degree of accuracy exhibited can be inadequate. To address this limitation, a more general form of the PDF was proposed in [21], by incorporating two additional "degrees-of-freedom"; that is, parameters to be determined based on an appropriate optimization scheme.

In this section, a more general form than Eq. (29) is proposed for the joint solution PDF of the system of coupled SDEs of Eq. (4). This can be construed as a generalization of the results of [21] to account for multi-dimensional processes $\mathbf{X}_t$. Specifically, the joint response transition PDF is expressed in the form

$$\hat{p}_{(\mathbf{k},\mathbf{n})}\left(\mathbf{x}_f, t_f|\mathbf{x}_i, t_i\right) = F_{(\mathbf{k},\mathbf{n})}(t_f)\exp\left(-G_{(\mathbf{k},\mathbf{n})}\left(\mathbf{x}_f, t_f|\mathbf{x}_i, t_i\right)\right), \tag{42}$$

where

$$(\mathbf{k},\mathbf{n}) = (k_1,\ldots,k_N,n_1,\ldots,n_N), \tag{43}$$

and

$$G_{(\mathbf{k},\mathbf{n})}\left(\mathbf{x}_f, t_f|\mathbf{x}_i, t_i\right) = \frac{\sum_{j=1}^{N}k_j\left(\chi^{(j)}\right)^2 + \sum_{j=1}^{N}n_j\left(-2M^{(j)}(\mathbf{x}_f)+2M^{(j)}(\mathbf{x}_i)\right)\tau}{2\tau\sigma^2}. \tag{44}$$

The constant F in Eq. (42) is determined as

$$F_{(\mathbf{k},\mathbf{n})}(t_f) = \left(\int_{\mathcal{D}(M)}\exp\left(-G_{(\mathbf{k},\mathbf{n})}\left(\mathbf{y}, t_f|\mathbf{x}_i, t_i\right)\right)d\mathbf{y}\right)^{-1}. \tag{45}$$

Note that in comparison to Eq. (29), the general solution form in Eq. (42) has $2N$ additional "degrees-of-freedom"; that is, the parameters $\mathbf{k}$ and $\mathbf{n}$ to be determined based on an appropriate optimization scheme. The rationale behind this choice relates to utilizing available knowledge and integrating it in an optimization scheme for determining Eq. (42), and thus, enhancing the overall accuracy of Eq. (29). In particular, the parameter $\mathbf{k}$ relates to optimizing and "tightening" the Cauchy–Schwarz inequality of Eq. (27), whereas the parameter $\mathbf{n}$ refers to the overall accuracy of the WPI approximation of Eq. (10). In comparison to Eq. (29) it is anticipated that the approximation of Eq. (42) will exhibit higher accuracy, at the expense of course of some added modest computational cost related to the optimization algorithm. In this regard, it is emphasized that exploiting a priori available information in many problems, such as obvious symmetries, can reduce significantly the effective size of the vector of unknown parameters $(\mathbf{k}, \mathbf{n})$. As seen also in many of the following numerical examples, the size of $(\mathbf{k}, \mathbf{n})$ can be considerably smaller than $2N$; thus, reducing the complexity and computational cost of the associated optimization problem.

Next, to determine the parameters $\mathbf{k}$ and $\mathbf{n}$ in Eq. (42), for a given norm $(\|\cdot\|_q)$, the error quantity of Eq. (37) is sought to be minimized; see also [21]. In fact, due to the closed-form expression of $\hat{p}_{(\mathbf{k},\mathbf{n})}$, the error quantity $err = \|\mathcal{L}_{FP}[\hat{p}_{(\mathbf{k},\mathbf{n})}]\|_q$ can be explicitly determined as a function of $\mathbf{k}$ and $\mathbf{n}$. Further, for a chosen q-norm and final time t_f, the values of $\mathbf{k}$, $\mathbf{n}$ are numerically evaluated by solving the optimization problem

$$\hat{z}_q = \left(\hat{\mathbf{k}}, \hat{\mathbf{n}}\right)_q = arg\min_{(\mathbf{k},\mathbf{n})\in\mathbb{R}^{2N}} err = arg\min_{(\mathbf{k},\mathbf{n})\in\mathbb{R}^{2N}}\|\mathcal{L}_{FP}[\hat{p}_{(\mathbf{k},\mathbf{n})}(\cdot,t_f)]\|_q, \tag{46}$$

and, thus, the approximate response PDF of Eq. (42), is determined. Note that in comparison to Section 3.3, in this section the closed-form expression of Eq. (37) is used not as an error estimate, but rather as a tool within the optimization scheme for enhancing the accuracy of the joint response PDF.

Table 1
Computed $(\mathbf{k}, \mathbf{n})$ values for various final time instants t_f and starting point (1,1,1,1) for Example 4.1.

	$k_1 = k_2$	$n_1 = n_2$	Iterations
$t_f = 0.1$	0.9848	0.4411	24
$t_f = 0.5$	1.0595	0.6001	36
$t_f = 1$	1.3648	0.8180	39
$t_f = 3$	3.4699	1.0824	36

Table 2
Error estimates and CPU times for Example 4.1.

	$\epsilon \times 10^{-4}$	ϵ_{ratio}	MCS CPU time (100,000 realizations)	$\hat{p}_{(\mathbf{k},\mathbf{n})}$ CPU time
$t_f = 0.1$	3.42	8.18	126 s	0.068 s
$t_f = 0.5$	3.92	23.20	534 s	0.081 s
$t_f = 1$	10	14.20	931 s	0.058 s
$t_f = 3$	17	23.23	2,313 s	0.051 s

4. Numerical examples

In the ensuing numerical examples, a standard interior point method [33,34] using Matlab's *fmincon* built-in function is employed to solve the unconstrained optimization problem of Eq. (46), in conjunction with the $\|\cdot\|_2$ norm (i.e., $q = 2$). To this aim, the basic approximation of Eq. (29) with $(\mathbf{k}, \mathbf{n}) = (1, \ldots, 1) \in \mathbb{R}^{2N}$ serves as a natural choice for the initial starting point of the algorithm.

In most of the numerical examples, the algorithm converged in less than a hundred iterations, which translates into less than a tenth of a second from a computational cost perspective for the examples considered. The accuracy of the approximate PDF of Eq. (42) is demonstrated by comparisons to the PDF estimated based on pertinent Euler-Maruyama MC simulation data (100,000 realizations) produced by numerically integrating the original Eq. (4) with $\Delta t = 10^{-2}$ on a computer with 16GB RAM, Inter(R) Core(TM) i7-6700 CPU @3.40GHz. Further, the error metric $\epsilon = \|\hat{p}_{(\mathbf{k},\mathbf{n})} - MCS\ PDF\|_2$ is employed for quantifying the accuracy of the approximate PDF as compared to the MC simulation based estimate. Also, the additional error quantity $\epsilon_{ratio} = \frac{\|\hat{p} - MCS\ PDF\|_2}{\|\hat{p}_{(\mathbf{k},\mathbf{n})} - MCS\ PDF\|_2}$ is utilized for demonstrating how much better the enhanced approximation $\hat{p}_{(\mathbf{k},\mathbf{n})}$ is in comparison to the basic one of $\hat{p}$.

4.1. Duffing kind nonlinearity: bimodal response PDF

In this example, a 2-dimensional Duffing nonlinear system with bimodal response PDF (e.g. [19]) of the form

$$\begin{cases} dX_t = (Y_t - X_t^3)dt + \sigma\, dB_t^{(1)} \\ dY_t = (X_t - Y_t^3)dt + \sigma\, dB_t^{(2)}, \end{cases} \tag{47}$$

is considered. Next, assuming zero initial conditions, and taking into account that $M_1(x, y) = xy - \frac{1}{4}x^4$ and $M_2(x, y) = M_1(y, x)$ the PDF of Eq. (42) takes the form

$$\hat{p}_{(\mathbf{k},\mathbf{n})}(x_f, y_f, t_f | 0, 0, 0) = F(t_f) \exp\left(- \frac{k_1 x_f^2 + k_2 y_f^2 - t_f\left(n_1\left(2x_f y_f - \frac{1}{2}x_f^4\right) + n_2\left(2x_f y_f - \frac{1}{2}y_f^4\right)\right)}{2t_f \sigma^2} \right). \tag{48}$$

Utilizing the parameter value $\sigma = 1$, and applying the numerical optimization scheme of Eq. (46) based on the $\|\cdot\|_2$ norm, yields the values for $(\mathbf{k}, \mathbf{n})$. Specifically, exploiting the symmetry of Eqs. (47) and (48) the number of the unknown parameters is reduced from four to two by setting $k_1 = k_2$ and $n_1 = n_2$. The computed values are shown in Table 1 along with the iterations number of the optimization algorithm, whereas in Table 2 error estimates and CPU times are presented as well. In Figs. 1–4 the approximate PDFs $\hat{p}_{(\mathbf{k},\mathbf{n})}$ of Eq. (48) are plotted for various time instants and compared both with the closed-form PDFs of Eq. (29) and with MCS based estimated PDFs. It is seen that the herein proposed enhanced PDF approximation of Eq. (48) is in very good agreement with MCS data, and yields improved performance as compared to the basic approximation of Eq. (29). Specifically, the closed-form basic approximation of Eq. (29) exhibits satisfactory accuracy at relatively early time instants, which deteriorates as t_f increases.

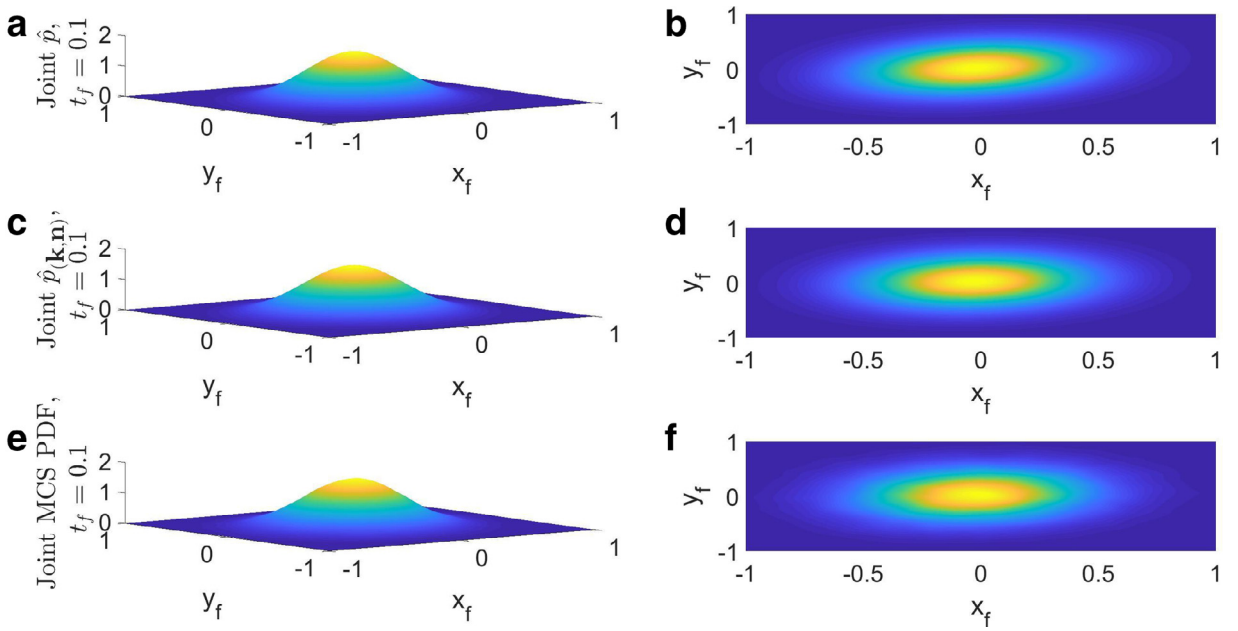

Fig. 1. Joint response PDF at $t_f = 0.1$ for a coupled system of SDEs with Duffing nonlinearity and bimodal response PDF: basic approximate PDF $\hat{p}$ (a) and (b); Enhanced approximate PDF $\hat{p}_{(\mathbf{k},\mathbf{n})}$ (c) and (d); MCS based PDF (100,000 realizations) (e) and (f).

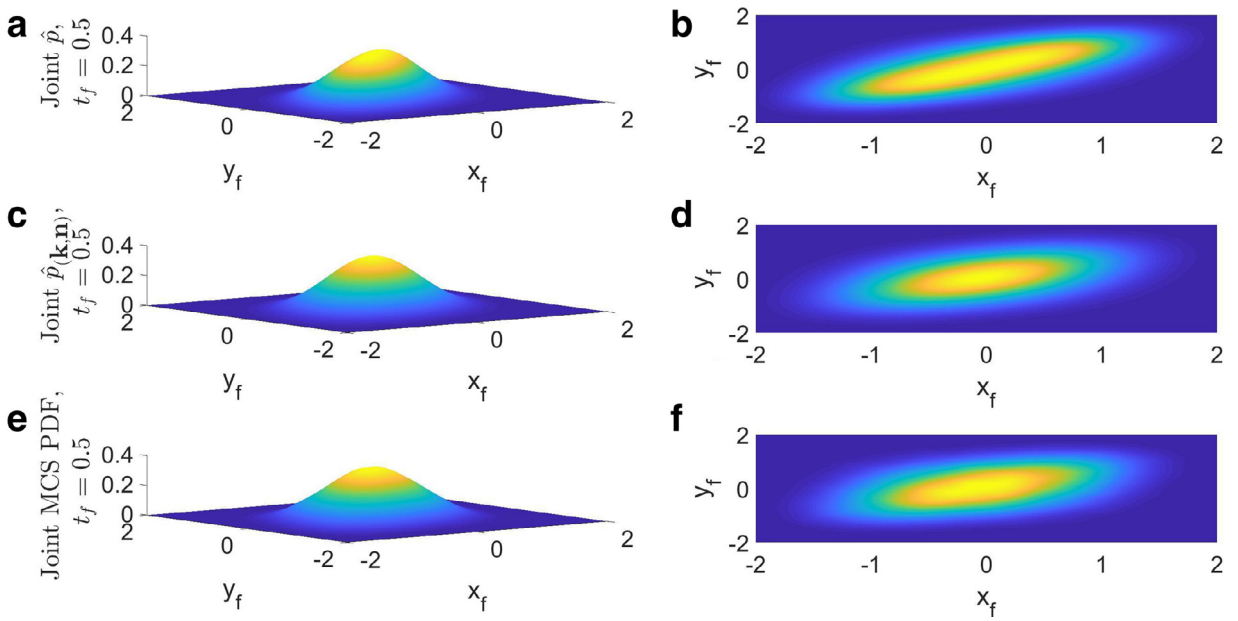

Fig. 2. Joint response PDF at $t_f = 0.5$ for a coupled system of SDEs with Duffing nonlinearity and bimodal response PDF: basic approximate PDF $\hat{p}$ (a) and (b); enhanced approximate PDF $\hat{p}_{(\mathbf{k},\mathbf{n})}$ (c) and (d); MCS based PDF (100,000 realizations) (e) and (f).

4.2. The "labyrinth" model

Let

$$s(i) = (i+1) \bmod N, \quad \forall i \in \mathbb{N}_0, \tag{49}$$

denote a circular shift permutation (rotation) operator of the natural numbers. The N-dimensional circulant system of the form

$$dX_t^{(j)} = \phi\left(X_t^{s^{\circ j}(0)}, X_t^{s^{\circ j}(1)}, \cdots, X_t^{s^{\circ j}(N-1)}\right)dt + \sigma\, dB_t^{(j)}, \quad \forall j \in \lceil N \rfloor, \tag{50}$$

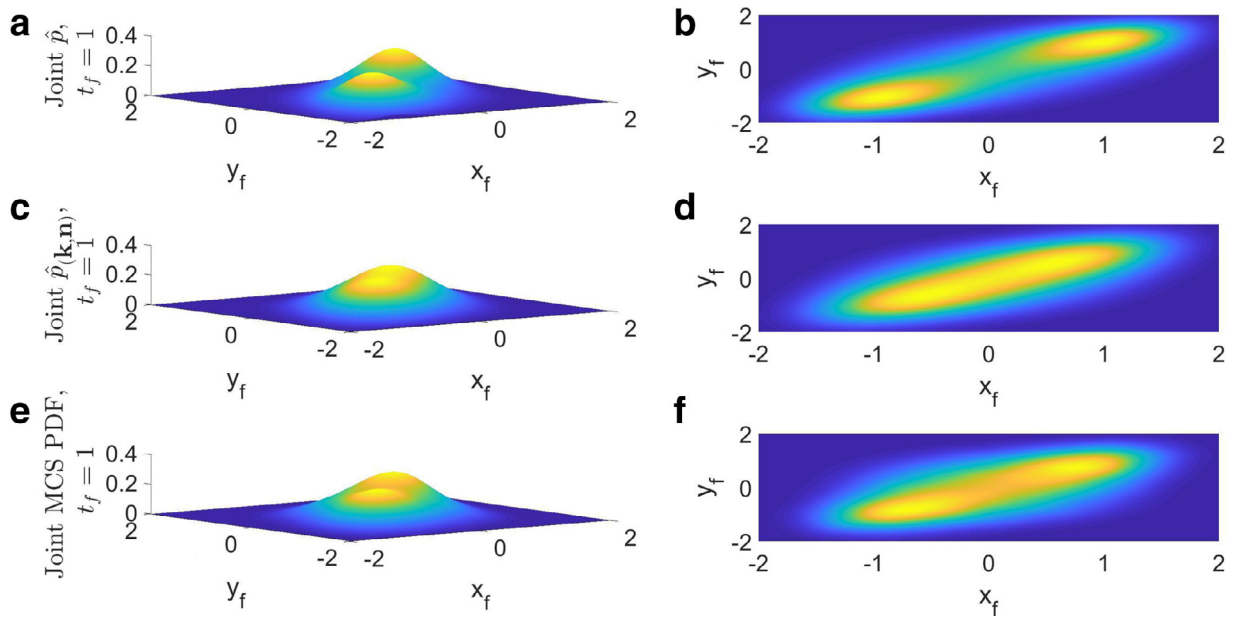

Fig. 3. Joint response PDF at $t_f = 1$ for a coupled system of SDEs with Duffing nonlinearity and bimodal response PDF: basic approximate PDF $\hat{p}$ (a) and (b); Enhanced approximate PDF $\hat{p}_{(\mathbf{k},\mathbf{n})}$ (c) and (d); MCS based PDF (100,000 realizations) (e) and (f).

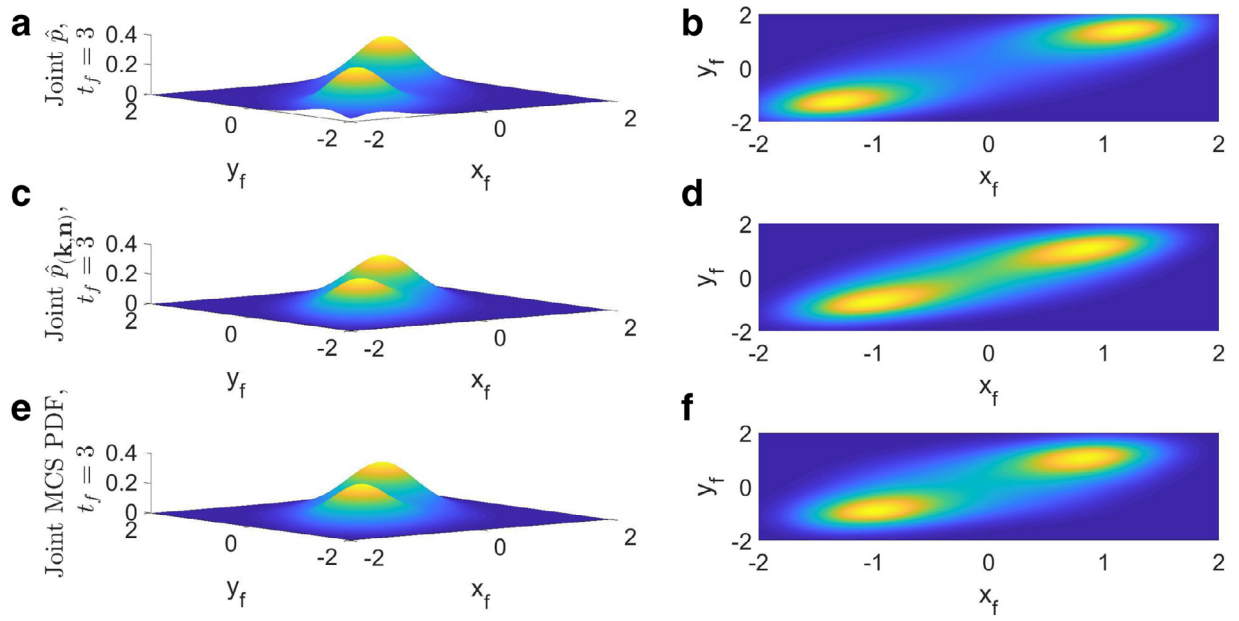

Fig. 4. Joint response PDF at $t_f = 3$ for a coupled system of SDEs with Duffing nonlinearity and bimodal response PDF: basic approximate PDF $\hat{p}$ (a) and (b); Enhanced approximate PDF $\hat{p}_{(\mathbf{k},\mathbf{n})}$ (c) and (d); MCS based PDF (100,000 realizations) (e) and (f).

where $s^{\circ j} = \overbrace{s \circ s \circ \cdots \circ s}^{j-times}$, for $\phi(a_1, a_2, \ldots, a_N) = sin(a_2)$, is typically called the labyrinth model [35–37], and has been used extensively in diverse applications [38–40] for representing auto-catalytic systems.

In the following example, a three-dimensional version of the labyrinth model given by Sprott [36]

$$\begin{cases} dX_t = \sin(Y_t)dt + \sigma\, dB_t^{(1)} \\ dY_t = \sin(Z_t)dt + \sigma\, dB_t^{(2)} \\ dZ_t = \sin(X_t)dt + \sigma\, dB_t^{(3)} \end{cases} \tag{51}$$

Table 3
Computed (**k**, **n**) values for various final time instants t_f and starting point (1,1,1,1,1,1) for Example 4.2.

	$k_1 = k_2 = k_3$	$n_1 = n_2 = n_3$	Iterations
$t_f = 0.5$	0.9594	0.2616	39
$t_f = 1$	0.8912	0.2680	27
$t_f = 10$	0.4376	0.0235	48
$t_f = 25$	0.4498	0.0068	57

Table 4
Error estimates and CPU times for Example 4.2.

	$\epsilon \times 10^{-4}$	MCS CPU time (100,000 realizations)	$\hat{p}_{(\mathbf{k},\mathbf{n})}$ CPU time
$t_f = 0.5$	0.74	974 s	0.036 s
$t_f = 1$	1.32	1687 s	0.025 s
$t_f = 10$	1.07	11, 923 s	0.027 s
$t_f = 25$	0.04	28, 369 s	0.085 s

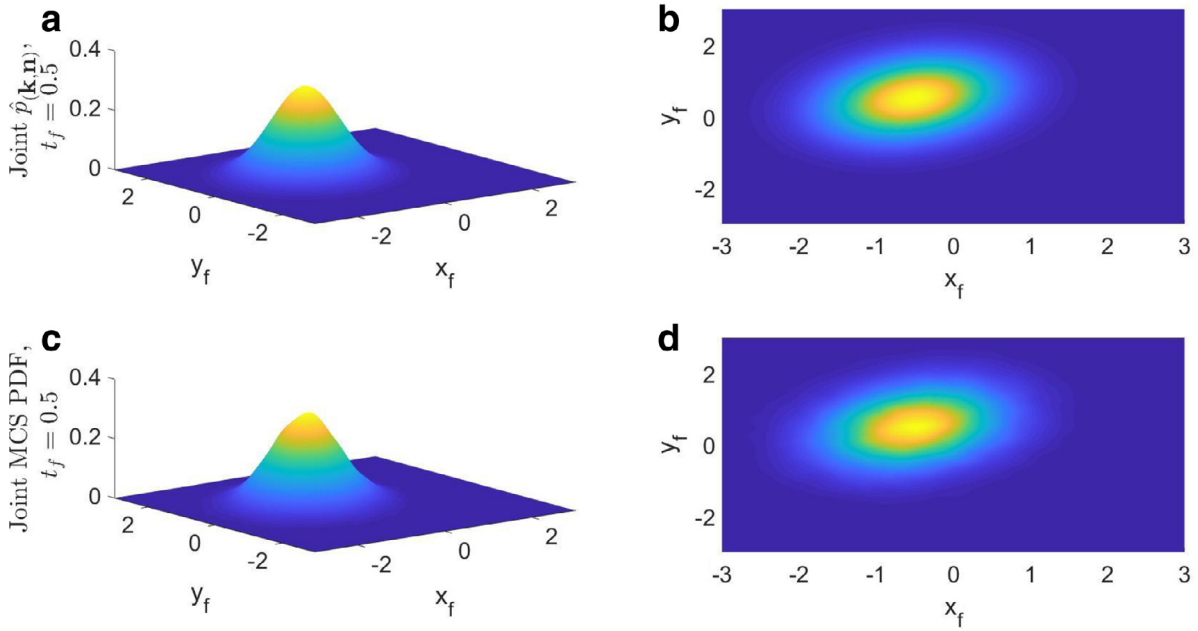

Fig. 5. Joint response PDF at $t_f = 0.5$ for a coupled nonlinear system of SDEs of the "labyrinth" type: Enhanced approximate PDF $\hat{p}_{(\mathbf{k},\mathbf{n})}$ (a) and (b); MCS based PDF (100,000 realizations) (c) and (d).

is utilized to assess the accuracy of the approximate response PDF of Eq. (42). Next, considering Eq. (51) and zero initial conditions, the PDF of Eq. (42) takes the form

$$\hat{p}_{(\mathbf{k},\mathbf{n})}(x_f, y_f, z_f, t_f|0,0,0,0) = F(t_f)\exp\left(-\frac{k_1x_f^2 + k_2y_f^2 + k_3z_f^2 + \left(-2n_1x_f\sin(y_f) - 2n_2y_f\sin(z_f) - 2n_3z_f\sin(x_f)\right)t_f}{2t_f\sigma^2}\right). \tag{52}$$

In the following, utilizing the parameter value $\sigma = 1$, and applying the numerical optimization scheme of Eq. (46) based on the $\|\cdot\|_2$ norm, yields the values for (**k**, **n**). Specifically, exploiting the symmetry of Eqs. (51) and (52) the number of the unknown parameters is reduced from six to two by setting $k_1 = k_2 = k_3$ and $n_1 = n_2 = n_3$. The computed values are shown in Table 3 along with the iterations taken by the optimization algorithm to converge, whereas in Table 4 error estimates and CPU times are included as well. In Figs. 5–8 the joint PDFs of X_t and Y_t are plotted for various time instants based on the

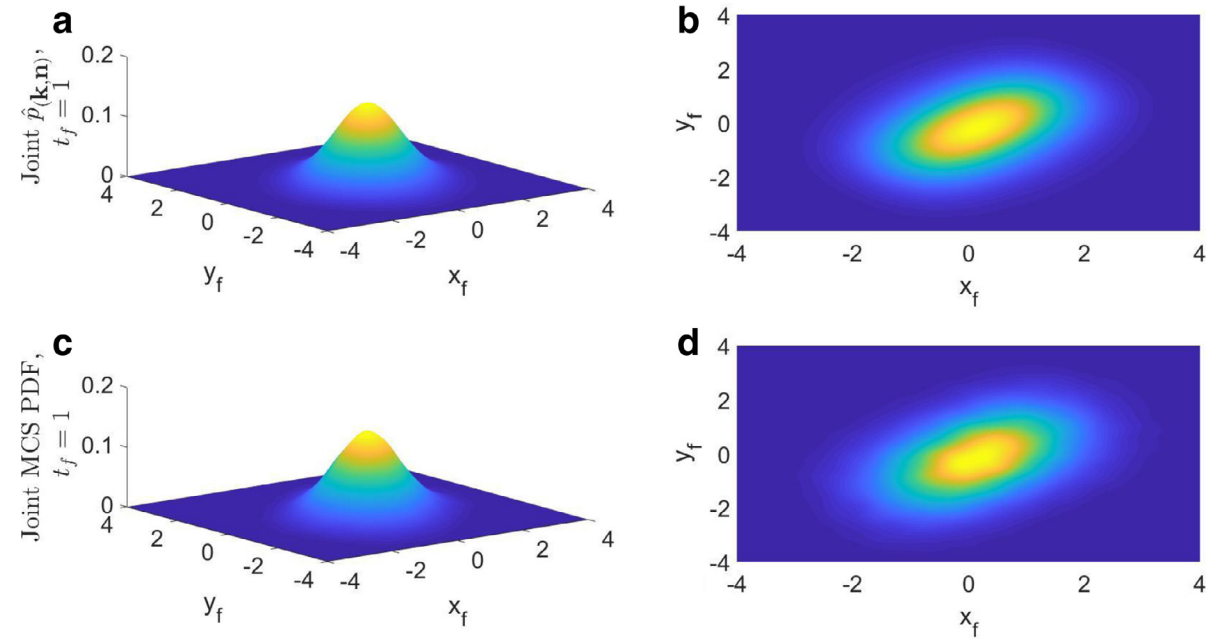

Fig. 6. Joint response PDF at $t_f = 1$ for a coupled nonlinear system of SDEs of the "labyrinth" type: Enhanced approximate PDF $\hat{p}_{(\mathbf{k},\mathbf{n})}$ (a) and (b); MCS based PDF (100,000 realizations) (c) and (d).

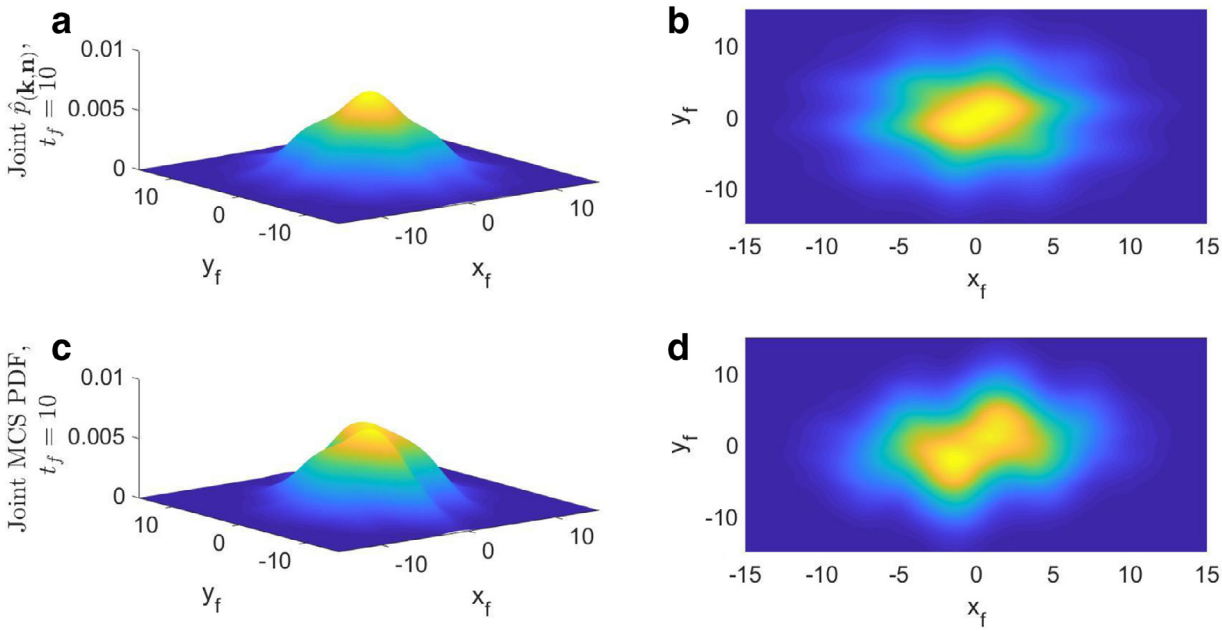

Fig. 7. Joint response PDF at $t_f = 10$ for a coupled nonlinear system of SDEs of the "labyrinth" type: Enhanced approximate PDF $\hat{p}_{(\mathbf{k},\mathbf{n})}$ (a) and (b); MCS based PDF (100,000 realizations) (c) and (d).

approximate PDFs $\hat{p}_{(\mathbf{k},\mathbf{n})}$ of Eq. (52) and compared with MCS based estimated PDFs. Additional results are shown in Fig. 9 corresponding to the marginal PDF of Z_t. It is seen that the herein proposed enhanced PDF approximation of Eq. (52) is in very good agreement with MC simulation data.

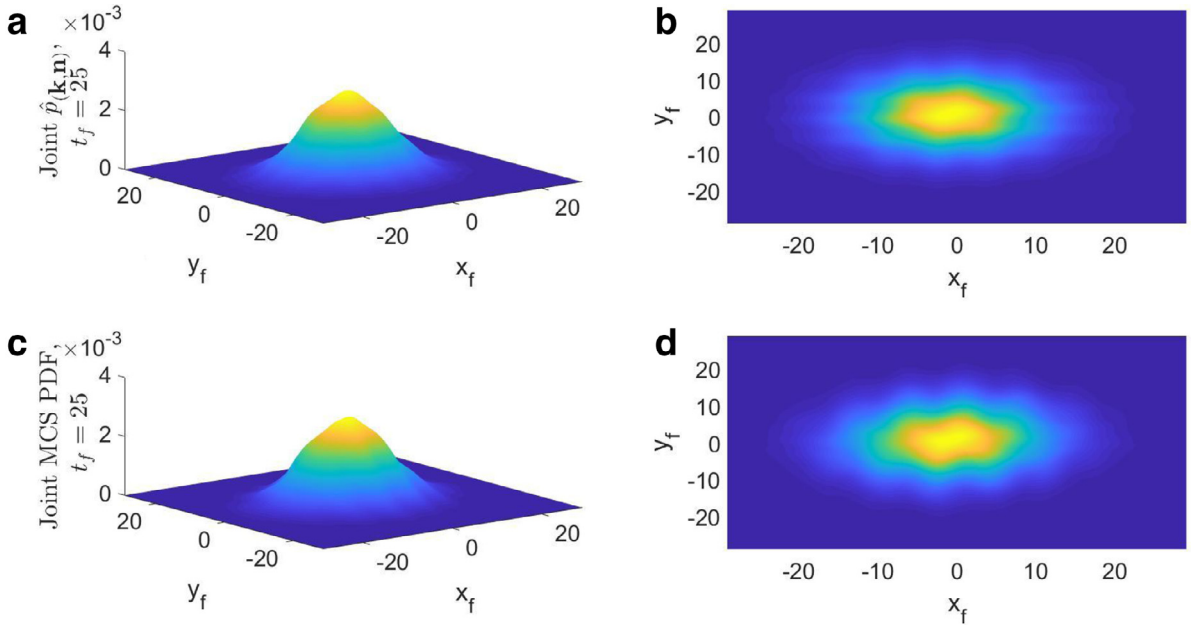

Fig. 8. Joint response PDF at $t_f = 25$ for a coupled nonlinear system of SDEs of the "labyrinth" type: Enhanced approximate PDF $\hat{p}_{(\mathbf{k},\mathbf{n})}$ (a) and (b); MCS based PDF (100,000 realizations) (c) and (d).

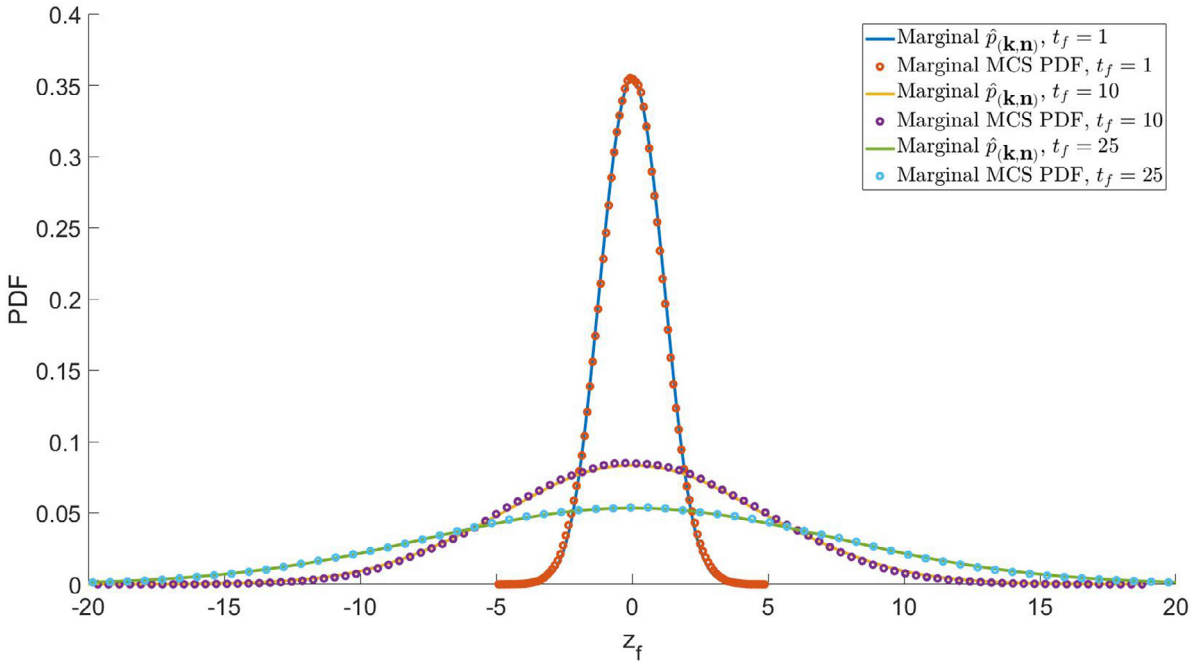

Fig. 9. Enhanced approximate marginal response PDFs $\hat{p}_{(\mathbf{k},\mathbf{n})}$ for various time instants t_f for a coupled nonlinear system of SDEs of the "labyrinth" type; comparisons with MCS based PDF estimates (100,000 realizations).

4.3. The predator-prey model

Various predator-prey mathematical models have been developed in ecology to describe the dynamics of species populations [41]. In this regard, a rather general predator-prey model is given by

$$\begin{cases} \dot{x}(t) = ax(t) - \phi(x(t))y(t) \\ \dot{y}(t) = -by(t) + c\phi(x(t))y(t), \end{cases} \tag{53}$$

Table 5
Computed ($\mathbf{k}$, $\mathbf{n}$) values for various final time instants t_f and starting point (1,1,1,1) for Example 4.3.

	k_1	k_2	n_1	n_2	Iterations
$t_f = 0.1$	0.9628	0.9667	2.8039	1.4113	100
$t_f = 0.5$	0.9406	0.9857	2.7976	1.4448	100
$t_f = 1$	0.9116	1.0421	2.5932	1.5088	120
$t_f = 10$	0.7614	1.5122	0.8480	2.3328	410

Table 6
Error statistics and CPU times for Example 4.3.

	$\epsilon \times 10^{-4}$	MCS CPU time (100,000 realizations)	$\hat{p}_{(\mathbf{k},\mathbf{n})}$ CPU time
$t_f = 0.1$	3.92	131 s	0.064 s
$t_f = 0.5$	1.44	520 s	0.059 s
$t_f = 1$	1.23	922 s	0.065 s
$t_f = 10$	3.16	13, 600 s	0.377 s

where $x(t)$, $y(t)$ represent the population densities of prey and predator, respectively; a, b and c are positive constants denoting the prey's intrinsic growth rate, the prey's death rate and the predator's conversion rate, respectively. Further, various expressions have been proposed in the literature for $\phi(x(t))$, ranging from Lotka–Volterra [41] to Holling-kind nonlinear modeling [42]. Without loss of generality, and following [43], a modified stochastic version of Leslie–Gower functional response and of the Holling-type II for the predator-prey model is given by

$$\begin{cases} dX_t = X_t\left(a - bX_t - \dfrac{cY_t}{m + X_t}\right)dt + \sigma X_t dB_t^{(1)} \\ dY_t = Y_t\left(r - \dfrac{fY_t}{m + X_t}\right)dt + \sigma Y_t dB_t^{(2)} \end{cases} \tag{54}$$

together with the initial conditions, $X(0) = X_0 > 0$, $Y(0) = Y_0 > 0$. In Eq. (54), the parameters a, b, c, r, f and m are all positive. These parameters are defined as follows: a is the growth rate of prey X, b measures the strength of competition among individuals of species X, c is the maximum value of the per capita reduction rate of X due to Y, m measures the extent to which the environment provides protection to prey X and to the predator Y, r describes the growth rate of Y and f has a similar meaning to c. The interested reader is referred to [44,45] for indicative generalizations of the model.

Next, setting $X = \exp(U)$ and $Y = \exp(V)$, Eq. (54) is cast in the form of Eq. (4); that is,

$$\begin{cases} dU_t = \left(a - \dfrac{\sigma^2}{2} - be^{U_t} - \dfrac{ce^{V_t}}{m + e^{U_t}}\right)dt + \sigma dB_t^{(1)} \\ dV_t = \left(r - \dfrac{\sigma^2}{2} - \dfrac{fe^{V_t}}{m + e^{U_t}}\right)dt + \sigma dB_t^{(2)} \end{cases} \tag{55}$$

and the PDF of Eq. (42) takes the form

$$\hat{p}_{(\mathbf{k},\mathbf{n})}(u_f, v_f, t_f | u_0, v_0, 0) = F(t_f) \exp\left(-\frac{k_1\left(u_f - u_0\right)^2 + k_2\left(v_f - v_0\right)^2}{2t_f\sigma^2}\right) \times \exp\left(-\frac{n_1\left(-M(u_f, v_f) + M(u_0, v_0)\right) + n_2\left(-K(u_f, v_f) + K(u_0, v_0)\right)}{\sigma^2}\right), \tag{56}$$

where $M(u, v) = au - \frac{\sigma^2}{2}u - be^u - \frac{ce^v(u - log(m + e^u))}{m}$ and $K(u, v) = rv - \frac{\sigma^2}{2}v - \frac{fe^v}{m + e^u}$.

In the numerical example, the parameter values $\sigma = 1$, $a = 0.4$, $b = 0.1$, $c = 0.1$, $r = 0.3$, $f = 0.5$, $m = 0.1$ are considered, together with the initial conditions $x_0 = y_0 = 0.3$. Next, applying the numerical optimization scheme of Eq. (46) based on the $\|\cdot\|_2$ norm yields the values for ($\mathbf{k}$, $\mathbf{n}$), which are shown in Eq. (5) along with the iterations number of the optimization algorithm, whereas in Table 6 error estimates and CPU times are presented for comparison purposes. In Figs. 10–13 the approximate PDFs $\hat{p}_{(\mathbf{k},\mathbf{n})}$ of Eq. (56) are plotted for various time instants and compared with MCS based estimated PDFs. It can be readily seen that the herein proposed enhanced PDF approximation of Eq. (56) exhibits satisfactory accuracy.

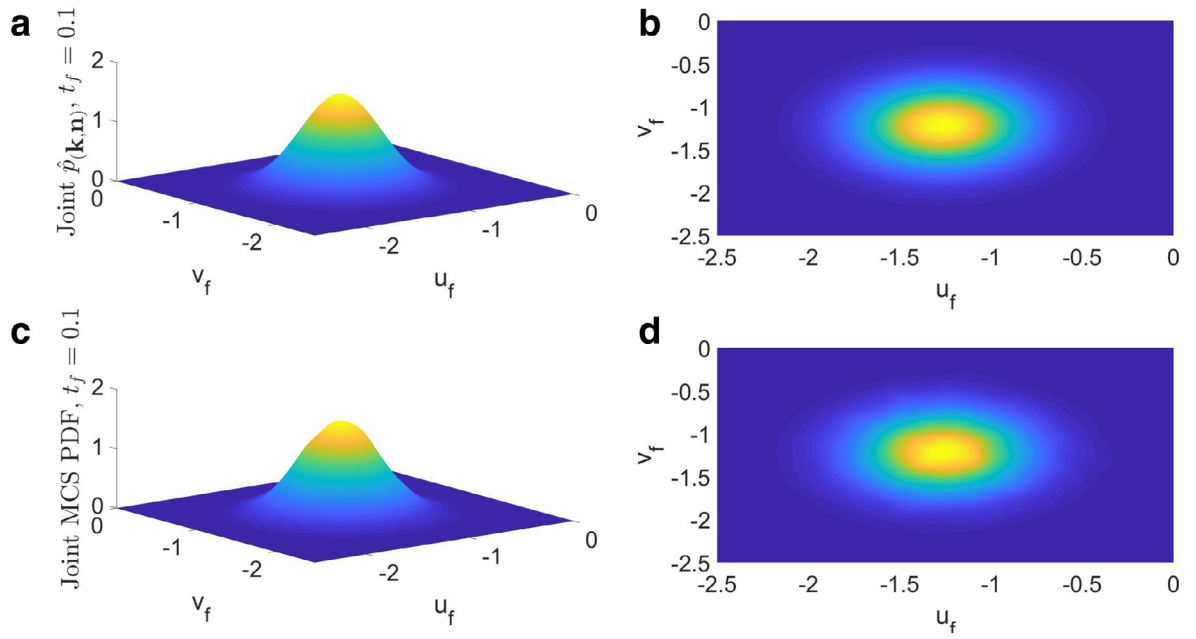

Fig. 10. Joint response PDF at $t_f = 0.1$ for a coupled predator-prey nonlinear system of SDEs: enhanced approximate PDF $\hat{p}_{(\mathbf{k},\mathbf{n})}$ (a) and (b); MCS based PDF (100,000 realizations) (c) and (d).

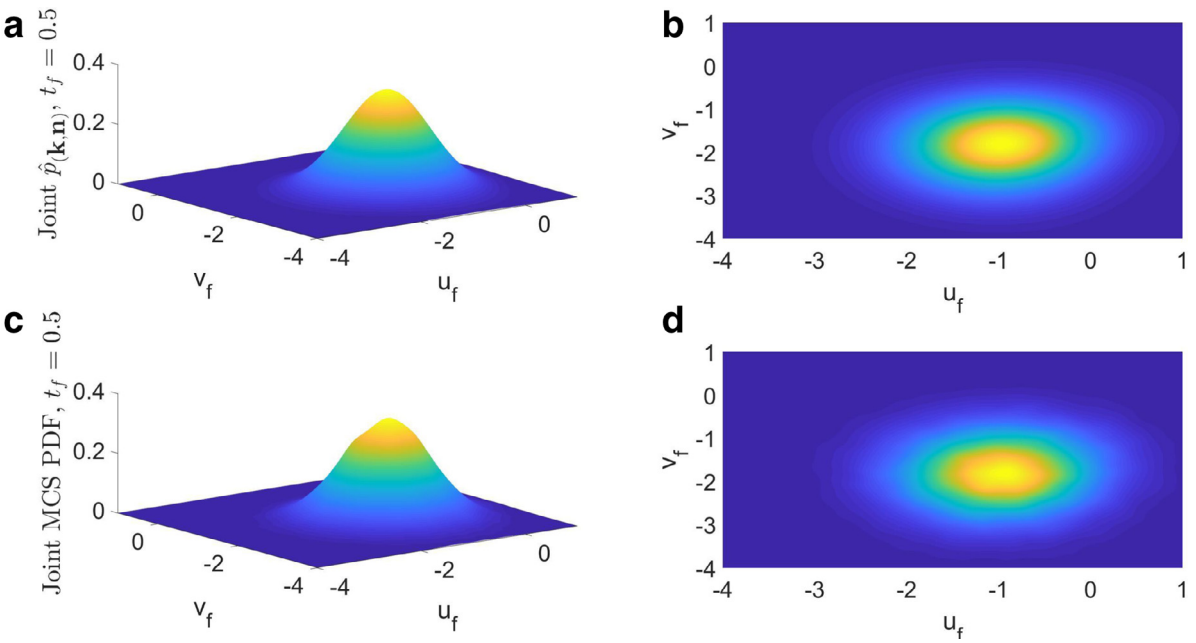

Fig. 11. Joint response PDF at $t_f = 0.5$ for a coupled predator-prey nonlinear system of SDEs: enhanced approximate PDF $\hat{p}_{(\mathbf{k},\mathbf{n})}$ (a) and (b); MCS based PDF (100,000 realizations) (c) and (d).

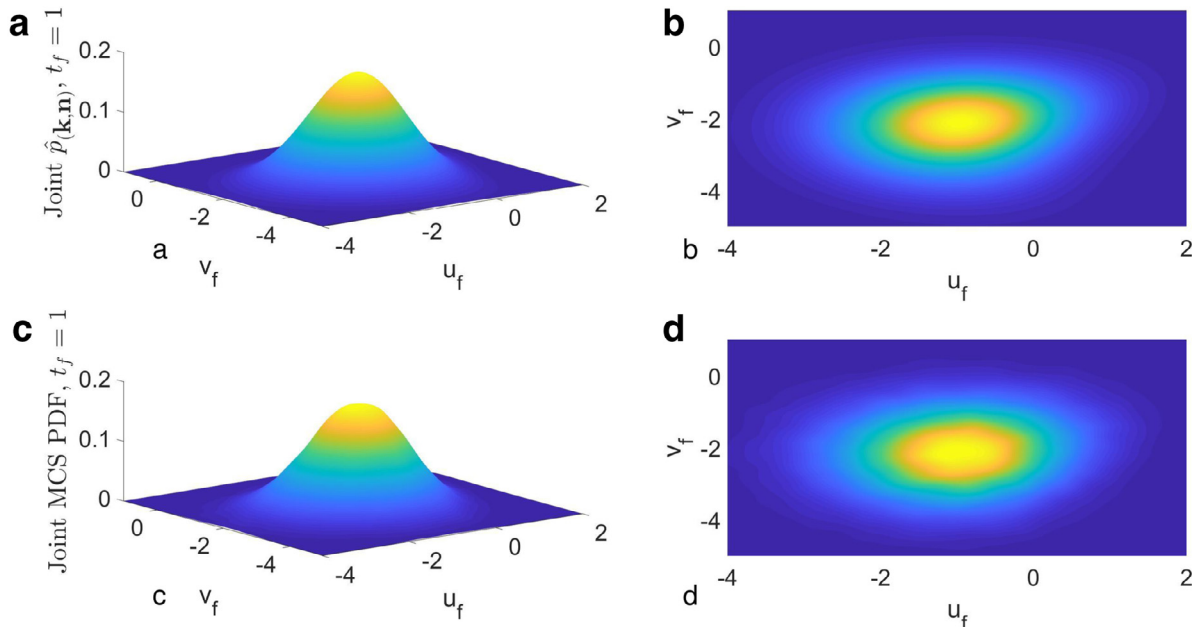

Fig. 12. Joint response PDF at $t_f = 1$ for a coupled predator-prey nonlinear system of SDEs: enhanced approximate PDF $\hat{p}_{(\mathbf{k},\mathbf{n})}$ (a) and (b); MCS based PDF (100,000 realizations) (c) and (d).

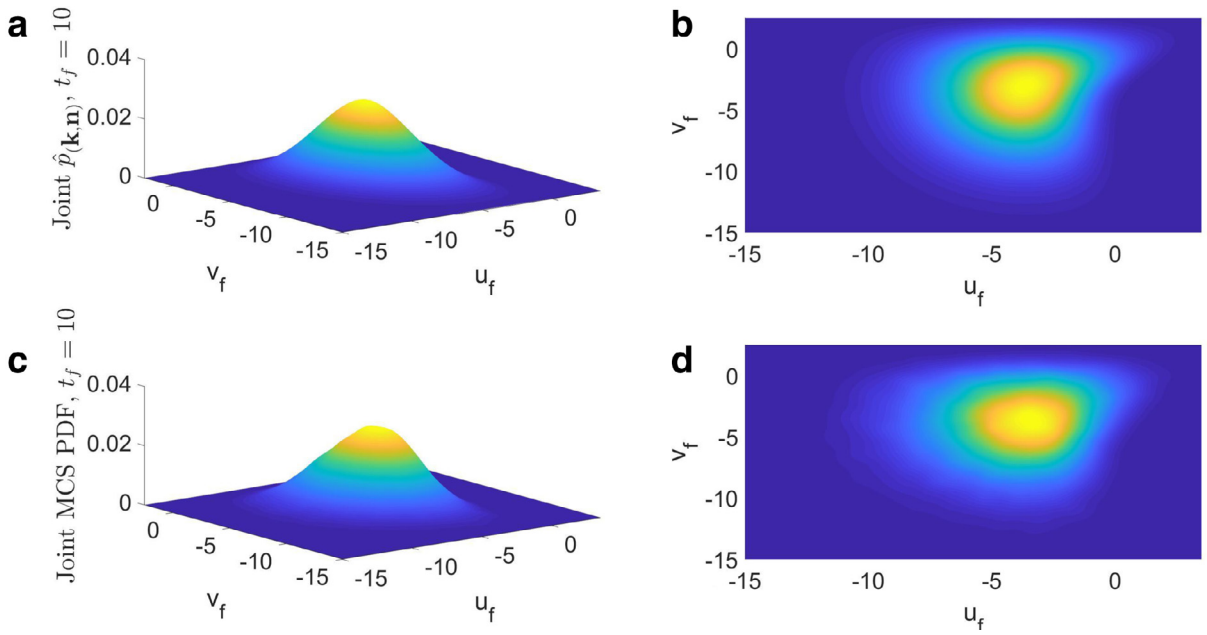

Fig. 13. Joint response PDF at $t_f = 10$ for a coupled predator-prey nonlinear system of SDEs: enhanced approximate PDF $\hat{p}_{(\mathbf{k},\mathbf{n})}$ (a) and (b); MCS based PDF (100,000 realizations) (c) and (d).

5. Conclusion

In this paper, an approximate analytical expression for the joint response transition PDF of a class of coupled SDEs with constant diffusion, but nonlinear drift coefficients, has been derived based on the concept of the Wiener path integral and on a Cauchy–Schwarz inequality treatment. Specifically, first, a basic approximation has been derived that requires essentially zero computational cost for its determination. Next, the approximation has been enhanced from an accuracy perspective by proposing a more general and versatile expression for the joint response transition PDF, which includes additional parameters. These are determined by formulating and solving an appropriate optimization problem related to

the corresponding Fokker–Planck equation. The enhanced PDF has demonstrated significant increase in accuracy, albeit at the expense of some modest computational cost related to the optimization scheme. Several diverse examples have been considered for assessing the reliability and accuracy of the derived approximation as compared to pertinent MC simulation data. In addition to the mathematical merit of the derived closed-form PDF, the approximate solutions can serve also as a benchmark for assessing the performance of alternative, more computationally demanding, stochastic dynamics numerical methodologies.

Acknowledgment

The authors would like to thank the Editor-in-Chief Theodore E. Simos and the anonymous reviewers for their insightful comments that significantly improved the quality of this paper. I. A. Kougioumtzoglou gratefully acknowledges the support through his CAREER award by the CMMI Division of the National Science Foundation, USA (Award number: 1748537).

References

[1] P.E. Kloeden, E. Platen, Numerical Solution of Stochastic Differential Equations, Springer-Verlag Berlin and Heidelberg Gmbh & Co. Kg, 1992.
[2] M. Grigoriu, Stochastic Calculus: Applications in Science and Engineering, Springer, New York, USA, 2002.
[3] S. Tronci, M. Grosso, J. Állvarez, R. Baratti, On the global nonlinear stochastic dynamical behavior of a class of exothermic CSTRs, J. Process Control 21 (9) (2011) 1250–1264.
[4] J. Álvarez, R. Baratti, S. Tronci, M. Grosso, A. Schaum, Global-nonlinear stochastic dynamics of a class of two-state two-parameter non-isothermal continuous stirred tank reactors, J. Process Control 72 (2018) 1–16.
[5] M.F. Wehner, W.G. Wolfer, Numerical evaluation of path-integral solutions to Fokker–Planck equations. II. Restricted stochastic processes, Phys. Rev. A 28 (5) (1983) 3003–3011.
[6] A. Naess, J.M. Johnsen, Response statistics of nonlinear, compliant offshore structures by the path integral solution method, Probab. Eng. Mech. 8 (2) (1993) 91–106.
[7] L. Chen, E.R. Jakobsen, A. Naess, On numerical density approximations of solutions of SDES with unbounded coefficients, Adv. Comput. Math. (2017) 1–29.
[8] J.B. Roberts, P.D. Spanos, Random Vibration and Statistical Linearization, Courier Corporation, 2003.
[9] J. Li, J. Chen, Stochastic Dynamics of Structures, John Wiley & Sons (Asia) Pte Ltd, 2009.
[10] N. Wiener, The average of an analytic functional and the Brownian movement, Proc. Natl. Acad. Sci. 7 (10) (1921) 294–298.
[11] R.P. Feynman, Space-time approach to non-relativistic quantum mechanics, Rev. Mod. Phys. 20 (2) (1948) 367.
[12] I.A. Kougioumtzoglou, P.D. Spanos, An analytical Wiener path integral technique for non-stationary response determination of nonlinear oscillators, Probab. Eng. Mech. 28 (2012) 125–131.
[13] I.A. Kougioumtzoglou, P.D. Spanos, Nonstationary stochastic response determination of nonlinear systems: a Wiener path integral formalism, ASCE J. Eng. Mech. 140 (9) (2014) 04014064.
[14] A. Di Matteo, I.A. Kougioumtzoglou, A. Pirrotta, P.D. Spanos, M. Di Paola, Stochastic response determination of nonlinear oscillators with fractional derivatives elements via the Wiener path integral, Probab. Eng. Mech. 38 (2014) 127–135.
[15] I.A. Kougioumtzoglou, A. Di Matteo, P.D. Spanos, A. Pirrotta, M. Di Paola, An efficient Wiener path integral technique formulation for stochastic response determination of nonlinear MDOF systems, ASME J. Appl. Mech. 82 (10) (2015) 101005.
[16] I.A. Kougioumtzoglou, A Wiener path integral solution treatment and effective material properties of a class of one-dimensional stochastic mechanics problems, ASCE J. Eng. Mech. 143 (6) (2017) 04017014.
[17] I. Petromichelakis, A.F. Psaros, I.A. Kougioumtzoglou, Stochastic response determination and optimization of a class of nonlinear electromechanical energy harvesters: A Wiener path integral approach, Probab. Eng. Mech. 53 (2018) 116–125.
[18] A.F. Psaros, O. Brudastova, G. Malara, I.A. Kougioumtzoglou, Wiener Path Integral based response determination of nonlinear systems subject to non-white, non-Gaussian, and non-stationary stochastic excitation, J. Sound Vib. 433 (2018) 314–333.
[19] A.F. Psaros, I.A. Kougioumtzoglou, I. Petromichelakis, Sparse representations and compressive sampling for enhancing the computational efficiency of the wiener path integral technique, Mech. Syst. Signal Process. 111 (2018) 87–101.
[20] A.T. Meimaris, I.A. Kougioumtzoglou, A.A. Pantelous, A closed form approximation and error quantification for the response transition probability density function of a class of stochastic differential equations, Probab. Eng. Mech. 54 (2018) 87–94.
[21] A.T. Meimaris, I.A. Kougioumtzoglou, A.A. Pantelous, Approximate analytical solutions for a class of nonlinear stochastic differential equations, Eur. J. Appl. Math. (2018) 1–17.
[22] T. Taniguchi, E.G.D. Cohen, Inertial effects in nonequilibrium work fluctuations by a path integral approach, J. Stat. Phys. 130 (1) (2008) 1–26.
[23] M. Chaichian, A. Demichev, Path Integrals in Physics: Volume I Stochastic Processes and Quantum Mechanics, CRC Press, 2001.
[24] R.L. Schilling, L. Partzsch, Brownian Motion: An Introduction to Stochastic Processes, Walter de Gruyter GmbH & Co KG, 2012.
[25] G.M. Ewing, Calculus of Variations with Applications, Dover Publications, New York, USA, 2016.
[26] J.M. Steele, The Cauchy–Schwarz Master Class: An Introduction to the Art of Mathematical Inequalities, Cambridge University Press, New York, USA, 2004.
[27] N.G. Van Kampen, Stochastic Processes in Physics and Chemistry, Elsevier, New York, USA, 2007.
[28] D. Kunszenti-Kovács, On the error of Fokker–Planck approximations of some one-step density dependent processes, arXiv:1612.08829, 2016.
[29] R. Grima, P. Thomas, A.V. Straube, How accurate are the nonlinear chemical Fokker–Planck and chemical Langevin equations? J. Chem. Phys. 135 (2011) 084103.
[30] Q. Yang, F. Liu, I. Turner, Stability and convergence of an effective numerical method for the time-space fractional Fokker–Planck equation with a nonlinear source term, Int. J. Diff. Eq. 2010 (2010) 1–22.
[31] H.A. Kramers, Brownian motion in a field of force and the diffusion model of chemical reactions, Physica 7 (4) (1940) 284–304.
[32] B. Øksendal, Stochastic Differential Equations: An Introduction with Applications, Springer-Verlag Berlin and Heidelberg Gmbh & Co. Kg, 2010.
[33] A. Forsgren, P.E. Gill, M.H. Wright, Interior methods for nonlinear optimization, SIAM Rev. 44 (4) (2002) 525–597.
[34] J. Nocedal, S. Wright, Numerical Optimization, Springer, New York, USA, 2006.
[35] R. Thomas, Deterministic chaos seen in terms of feedback circuits: analysis, synthesis, "labyrinth chaos", Int. J. Bifurc. Chaos 9 (10) (1999) 1889–1905.
[36] J.C. Sprott, Elegant Chaos: Algebraically Simple Chaotic Flows, World Scientific, Singapore., 2010.
[37] S. Vaidyanathan, C. Volos, Advances and Applications in Chaotic Systems, Springer-Verlag Berlin and Heidelberg Gmbh & Co. Kg, 2016.
[38] S. Rasmussen, C. Knudsen, R. Feldberg, M. Hindsholm, The coreworld: emergence and evolution of cooperative structures in a computational chemistry, Phys. D: Nonlinear Phenom. 42 (1–3) (1990) 111–134.
[39] J.L. Deneubourg, S. Goss, Collective patterns and decision-making, Ethol. Ecol. Evol. 1 (1989) 295–311.
[40] S.A. Kauffman, The Origins of Order: Self-Organization and Selection in Evolution, Oxford University Press, USA, 1993.
[41] H.I. Freedman, Deterministic Mathematical Models in Population Ecology, Pure and applied mathematics, Marcel Dekker, Inc., New York, USA, 1980.

[42] B. Liu, Z. Teng, L. Chen, Analysis of a predator–prey model with Holling II functional response concerning impulsive control strategy, J. Comput. Appl. Math. 193 (2006) 347–362.
[43] C. Ji, D. Jiang, N. Shi, Analysis of a predator–prey model with modified Leslie–Gower and Holling-type II schemes with stochastic perturbation, J. Math. Anal. Appl. 359 (2) (2009) 482–498.
[44] A.F. Nindjin, M.A. Aziz-Alaoui, M. Cadivel, Analysis of a predator–prey model with modified Leslie–Gower and Holling-type II schemes with time delay, Nonlinear Anal.: Real World Appl. 7 (2006) 1104–1118.
[45] H. Guo, X. Song, An impulsive predator–prey system with modified Leslie–Gower and Holling type II schemes, Chaos Solitons Fractals 36 (5) (2008) 1320–1331.